Advances in Applied Mathematics and Mechanics
Adv. Appl. Math. Mech., Vol. **18**, No. 1, pp. 296-321

DOI: 10.4208/aamm.OA-2024-0117
February 2026

Meshfree Methods for the Helmholtz Equation with Variable Wave Speed

Zhiyong Liu and Qiuyan Xu*

School of Mathematics and statistics, Ningxia University, Yinchuan, Ningxia 750021, China

Received 3 June 2024; Accepted (in revised version) 31 October 2024

Abstract. In this paper, we develop one-level and multilevel meshfree radial basis functions (RBF) collocation methods for solving the Helmholtz equation with variable wave speed on a bounded connected Lipschitz domain. The approximate solution is constructed by employing successive refinement scattered data sets and scaled compactly supported radial basis functions with varying support radii. We prove the convergence of one-level and multilevel collocation method for the modelling problem in Sobolev spaces. The convergence rates depend on the regularity of the solution, the smoothness of the computational domain, the bounds of frequency and wave speed, the approximation of scaled kernel-based spaces, the increasing rules of scattered data, and the selection of scaling parameters.

AMS subject classifications: 65N12, 65N15, 65N35

Key words: Helmholtz equation, radial basis functions, meshfree methods, collocation, variable wave speed.

1 Introduction

The Helmholtz equation has many important applications, including time-harmonic acoustic wave-propagation, radar and sonar detection as well as medical and seismic imaging, and so on. A general Helmholtz equation in heterogeneous media has the form

$$-\operatorname{div}(a(\boldsymbol{x})\operatorname{grad} u)-\left(\frac{\omega}{c(\boldsymbol{x})}\right)^2 u=f(\boldsymbol{x}) \qquad \text{in } \Omega, \tag{1.1a}$$

$$a(\boldsymbol{x})\frac{\partial u}{\partial \boldsymbol{n}}-i\omega\beta(\boldsymbol{x})u=g(\boldsymbol{x}) \qquad \text{on } \partial\Omega. \tag{1.1b}$$

*Corresponding author.
Emails: zhiyong@nxu.edu.cn (Z. Liu), qiuyanxu@nxu.edu.cn (Q. Xu)

Where $\Omega \subset \mathbb{R}^d$ is a bounded Lipschitz domain, frequency $\omega \geq \omega_0 > 0$. For the coefficients, we suppose $a(\boldsymbol{x}), c(\boldsymbol{x})$ are bounded above and below by strictly positive numbers, real-valued $\beta(\boldsymbol{x}) \in L^\infty(\partial\Omega)$. It's usually assumed that $f \in L^2(\Omega)$ and $g \in L^2(\partial\Omega)$ (or weaker assumption $g \in H^{-1/2}(\partial\Omega)$).

Several grid-type numerical methods have been designed to solve the Helmholtz equation, such as finite difference methods [3, 10, 11] and finite element methods [5, 17, 21, 31]. To avoid mesh generation in complex domain, the radial basis functions has been gradually used for numerical solution of Helmholtz equation [22, 26]. The radial basis functions allow the easy construction of approximation spaces in arbitrary dimensions with arbitrary smoothness. Therefore, this paper will consider one-level and multilevel radial basis collocation methods for the Helmholtz equation with variable wave speed.

The paper is organized as follows. Section 2 is devoted to some notation in Sobolev spaces. Section 3 discusses the well-posedness of Helmholtz equation and its priori bounds. Sections 4 and 5 provide the convergence of one-level collocation method and multilevel collocation method respectively. Section 6 gives several numerical examples and deals with numerical efficiency. The paper ends with some concluding remarks in Section 7.

2 Preliminaries

2.1 Sobolev space on Ω

When considering some complex-valued functions, we denote the scalar product and norm of $L^2(\Omega)$ as

$$(u,v) = \int_\Omega u\overline{v} d\boldsymbol{x}, \quad \|u\|_{L^2(\Omega)} = \left(\int_\Omega u\overline{u} d\boldsymbol{x} \right)^{1/2}, \quad u,v \in L^2(\Omega).$$

With a nonnegative integer k, Sobolev space $W^{k,2}(\Omega)$ contains all functions which have weak differentiability order k and integrability power 2. $W^{k,2}(\Omega)$ has been assembled with the (semi-) norms

$$|u|_{W^{k,2}(\Omega)} = \left(\sum_{|\alpha|=k} \|D^\alpha u\|^2_{L^2(\Omega)} \right)^{1/2}, \quad \|u\|_{W^{k,2}(\Omega)} = \left(\sum_{|\alpha|\leq k} \|D^\alpha u\|^2_{L^2(\Omega)} \right)^{1/2}.$$

$W^{k,\infty}(\Omega)$ (semi-) norms are defined as

$$|u|_{W^{k,\infty}(\Omega)} = \sup_{|\alpha|=k} \|D^\alpha u\|_{L^\infty(\Omega)}, \quad \|u\|_{W^{k,\infty}(\Omega)} = \sup_{|\alpha|\leq k} \|D^\alpha u\|_{L^\infty(\Omega)}.$$

Because $W^{k,2}(\Omega)$ is a Hilbert space, we usually denote $W^{k,2}(\Omega)$ as $H^k(\Omega)$. With a non-integer values $0 < \sigma < \infty$, the fractional order Sobolev space $H^\sigma(\mathbb{R}^d)$ is characterized by Fourier transform

$$\widehat{u}(\boldsymbol{\omega}) = (2\pi)^{-d/2} \int_{\mathbb{R}^d} u(\boldsymbol{x}) e^{-i\boldsymbol{x}^T\boldsymbol{\omega}} d\boldsymbol{x}. \tag{2.1}$$

At this time the norm of $H^\sigma(\mathbb{R}^d)$ is given by

$$\|u\|^2_{H^\sigma(\mathbb{R}^d)} = \int_{\mathbb{R}^d} |\widehat{u}(\boldsymbol{\omega})|^2 (1+\|\boldsymbol{\omega}\|_2^2)^\sigma d\boldsymbol{\omega}. \tag{2.2}$$

$H^\sigma(\Omega)$ is a subspace of $H^\sigma(\mathbb{R}^d)$, which can be simply defined by

$$H^\sigma(\Omega) = \{u|_\Omega : u \in H^\sigma(\mathbb{R}^d)\}.$$

Definition 2.1. *We say Ω has a Lipschitz boundary $\partial\Omega$ provided there exists a collection of open sets O_i, a positive parameter ϵ, an integer N and a finite number M, such that for all $\boldsymbol{x} \in \partial\Omega$ the ball of radius ϵ centered at $\boldsymbol{x}$ is contained in some O_i, no more than N of the sets O_i intersect nontrivially, and each domain $O_i \cap \Omega = O_i \cap \Omega_i$, where Ω_i is a domain whose boundary is a graph of a Lipschitz function ϕ_i (i.e., $\Omega_i = \{(\boldsymbol{x},\boldsymbol{y}) \in \mathbb{R}^d : \boldsymbol{x} \in \mathbb{R}^{d-1}, \boldsymbol{y} < \phi_i(\boldsymbol{x}))\}$) satisfying $\|\phi_i\|_{Lip(\mathbb{R}^{d-1})} \leq M$.*

With the Definition of Lipschitz boundary [4], the connection between $H^\sigma(\Omega)$ and $H^\sigma(\mathbb{R}^d)$ can be characterized by Sobolev extension [1].

Lemma 2.1 (Sobolev extension)**.** *Let $\Omega \subseteq \mathbb{R}^d$ be open and have a Lipschitz boundary. Let $\sigma \geq 0$. Then there exists a linear operator $E : H^\sigma(\Omega) \to H^\sigma(\mathbb{R}^d)$ such that for all $f \in H^\sigma(\Omega)$ the following results hold:*

(1). $Ef|_\Omega = f$,

(2). $\|Ef\|_{H^\sigma(\mathbb{R}^d)} \leq C\|f\|_{H^\sigma(\Omega)}$.

2.2 Sobolev space on $\partial\Omega$

The scalar product and norm of $L^2(\partial\Omega)$ can be defined as

$$(u,v)_{\partial\Omega} = \int_{\partial\Omega} u\overline{v} ds, \quad \|u\|_{L^2(\partial\Omega)} = \left(\int_{\partial\Omega} u\overline{u} ds\right)^{1/2}, \quad u,v \in L^2(\partial\Omega).$$

If Ω has a $C^{k,s}-$boundary with $s \in [0,1)$, then we can define the Sobolev norm on $\partial\Omega$ by a number of $C^{k,s}-$diffeomorphisms

$$\psi_j : B \to V_j, \quad 1 \leq j \leq K,$$

where $B = B(\mathbf{0},1)$ is the unit ball in $\mathbb{R}^{d-1}$ and $V_j \subseteq \mathbb{R}^d$ are open sets such that $\partial\Omega = \bigcup_{j=1}^K V_j$. Hence the Sobolev norm on the boundary can be defined by

$$\|u\|^2_{H^\sigma(\partial\Omega)} = \sum_{j=1}^K \|(u\omega_j)\circ\psi_j\|^2_{H^\sigma(B)},$$

where $\{\omega_j\}$ is a partition of unity with respect to V_j. When $\sigma = 0$, we discuss the relationship between $L^2(\partial\Omega)$ and $H^0(\partial\Omega)$. This is the following lemma. An early version can be found in the book [38].

Lemma 2.2. *Suppose $\Omega\subseteq\mathbb{R}^d$ is a bounded domain with $C^{k,s}-$boundary. Then, there exists a constant C such that*

$$\|u\|_{L^2(\partial\Omega)}\leq C\|u\|_{H^0(\partial\Omega)}.$$

Proof. By the definition of $L^2(\partial\Omega)$ and the partition of unity, we have

$$\begin{aligned}\|u\|^2_{L^2(\partial\Omega)}=&\int_{\partial\Omega}|u|^2ds=\sum_{j=1}^K\int_{\partial\Omega}|u\omega_j|^2ds=\sum_{j=1}^K\int_{V_j\cap\partial\Omega}|u\omega_j|^2ds\\=&\sum_{j=1}^K\int_B|(u\omega_j)\circ\psi_j|^2\cdot|J_j(\boldsymbol{y})|d\boldsymbol{y}\leq C\sum_{j=1}^K\int_B|(u\omega_j)\circ\psi_j|^2d\boldsymbol{y}\\=&C\sum_{j=1}^K\|(u\omega_j)\circ\psi_j\|^2_{H^0(B)}=C\|u\|^2_{H^0(\partial\Omega)}.\end{aligned}$$

Where, $\boldsymbol{y}\in\mathbb{R}^{d-1}$, and $J_j(\boldsymbol{y})$ are some Jacobi matrices. Because Ω has $C^{k,s}-$boundary, by Paragraph 4.10 in [1] we know $|J_j(\boldsymbol{y})|$ are bounded. □

To establish a relationship between Sobolev norm for the domain Ω and Sobolev norm for the boundary $\partial\Omega$, we need to cite the trace theorem and inverse trace theorem.

Lemma 2.3 (Trace theorem)**.** *Suppose $\Omega\subseteq\mathbb{R}^d$ is a bounded domain with $C^{k,s}-$boundary. Let $1/2<\sigma<k+s$. Then, there exists a continuous linear operator*

$$T:H^\sigma(\Omega)\to H^{\sigma-1/2}(\partial\Omega),$$

such that $Tu=u|_{\partial\Omega}$ for all $u\in H^\sigma(\Omega)$ and

$$\|u\|_{H^{\sigma-1/2}(\partial\Omega)}\leq C\|u\|_{H^\sigma(\Omega)}$$

for some positive constant C, which is independent of u.

The proof of trace theorem can be found in [39]. The following inverse trace theorem depicts the opposite situation, namely, the linear mapping from $H^{\sigma-1/2}(\partial\Omega)$ to $H^\sigma(\Omega)$.

Lemma 2.4 (Inverse Trace theorem)**.** *Suppose $\Omega\subseteq\mathbb{R}^d$ is a bounded region with $C^{k,s}-$boundary. Let $1/2<\sigma<k+s$. Then, there exists a continuous linear operator*

$$Z:H^{\sigma-1/2}(\partial\Omega)\to H^\sigma(\Omega),$$

such that $T\circ Zu=u$ for all $u\in H^{\sigma-1/2}(\partial\Omega)$.

3 Helmholtz equation

One priori bounds or well-posedness of the Helmholtz equation plays an important role in theoretical analysis of numerical methods. The analysis of convergence of radial basis functions collocation method is also closely dependent on the priori bounds. The earlier stability estimate for the heterogeneous Helmholtz equation goes back to [2]. Unfortunately, the explicit stability for the Helmholtz equation in heterogeneous media with the general form (1.1a)-(1.1b) is very rare [5,16,17,28].

We use the regularity result from [5].

Theorem 3.1 (Regularity). *Suppose $\Omega\subset\mathbb{R}^d$ is a bounded connected Lipschitz domain and satisfies the geometric assumptions in [18]. And suppose there exist positive constants $a_{\min}$, $a_{\max}$, $c_{\min}$, $c_{\max}$, $\beta_{\min}$, $\beta_{\max}$, such that for all $x\in\Omega$,*

$$a_{\min}\le a(\boldsymbol{x})\le a_{\max},\quad c_{\min}\le c(\boldsymbol{x})\le c_{\max},\quad \beta_{\min}\le\beta(\boldsymbol{x})\le\beta_{\max}.$$

Further, we suppose u has the regularity $u\in H^{3/2+\delta}(\Omega)$ for some $\delta>0$. Define a function

$$s(\boldsymbol{x}):=div\left(\frac{1}{a(\boldsymbol{x})c^2(\boldsymbol{x})}(\boldsymbol{x}-\boldsymbol{x}_0)\right),$$

and denote C to be the minimal constant such that

$$2\left|\int_\Omega\left(\frac{\nabla a(\boldsymbol{x})}{a(\boldsymbol{x})}\right)\nabla u((\boldsymbol{x}-\boldsymbol{x}_0)\cdot\nabla\overline{u})dx\right|\le C\left\|\frac{\nabla a(\boldsymbol{x})}{a(\boldsymbol{x})}\right\|_{L^\infty(\Omega)}\|\nabla u\|^2_{L^2(\Omega)}.$$

Furthermore, we suppose that

$$\begin{aligned}&s_{\min}=\min_{\boldsymbol{x}\in\Omega}s(\boldsymbol{x})>0,\\&s_{\min}-\left((d-2)+C\left\|\frac{\nabla a(\boldsymbol{x})}{a(\boldsymbol{x})}\right\|_{L^\infty(\Omega)}\right)\frac{1}{a_{\min}c^2_{\min}}>0.\end{aligned}$$

Then, the following estimate holds

$$\left\|\sqrt{a(\boldsymbol{x})}\nabla u\right\|^2_{L^2(\Omega)}+\left\|\frac{\omega}{c(\boldsymbol{x})}u\right\|^2_{L^2(\Omega)}\le C^*\left(1+\frac{1}{\omega^2}\right)\left(\|f\|^2_{L^2(\Omega)}+\|g\|^2_{L^2(\partial\Omega)}\right),\tag{3.1}$$

here C^* is independent of ω.

For the convenience of subsequent theoretical analysis, we set

$$a(\boldsymbol{x})=1,\quad \beta(\boldsymbol{x})=\frac{1}{c(\boldsymbol{x})}.$$

Define the two linear differential operators

$$Lu := -\Delta u - \left(\frac{\omega}{c(\boldsymbol{x})}\right)^2 u, \quad Bu := \frac{\partial u}{\partial \boldsymbol{n}} - i\frac{\omega}{c(\boldsymbol{x})}u.$$

Then (1.1a)-(1.1b) can be reduced to

$$Lu = f(\boldsymbol{x}) \qquad \text{in } \Omega, \tag{3.2a}$$
$$Bu = g(\boldsymbol{x}) \qquad \text{on } \partial\Omega. \tag{3.2b}$$

We can derive a priori bounds of (3.2a)-(3.2b) to form the following theorem.

Theorem 3.2 (A priori bounds). *Let $\Omega \subset \mathbb{R}^d$ $(d = 1,2,3)$ be a bounded connected Lipschitz domain. Let the frequency $\omega \geq \omega_0 > 0$. Let $c(\boldsymbol{x}) \in L^\infty(\Omega)$ be bounded by*

$$0 < c_{\min} \leq c(\boldsymbol{x}) \leq c_{\max} < \infty.$$

Under the same assumption as Theorem 3.1. *Then there exist positive C_{stab} which depends on ω such that*

$$\|u\|^2_{L^2(\Omega)} \leq C_{stab} \cdot \frac{c_{\max}}{\omega}\left(\|f\|^2_{L^2(\Omega)} + \|g\|^2_{L^2(\partial\Omega)}\right). \tag{3.3}$$

In the later discussion, we always assume that the conditions of Theorem 3.2 are satisfied. Then, we can characterize the continuity of Helmholtz operator and boundary differential operator.

Lemma 3.1 (Continuity of L and B). *Let $\sigma \in \mathbb{R}$, and $k = \lfloor \sigma \rfloor > d/2+2$. Let $c(\boldsymbol{x}) \in W^{k-1,\infty}(\Omega)$. Suppose the solution of* (3.2a)-(3.2b) *has the regularity $u \in H^\sigma(\Omega)$. Then L and B both are bounded operators which satisfy*

$$\|Lu\|_{H^{\sigma-2}(\Omega)} \leq C\omega^2 \|u\|_{H^\sigma(\Omega)},$$
$$\|Bu\|_{L^2(\partial\Omega)} \leq C\frac{\omega}{c_{\min}} \|u\|_{H^1(\partial\Omega)}.$$

Proof. Take a multi-index $\alpha \in \mathbb{N}_0^d$ with $|\alpha| \leq k-1$, then we have

$$\begin{aligned}\left|D^\alpha\left(\frac{\omega}{c(\boldsymbol{x})}\right)^2 u\right| &= \omega^2 \left|\sum_{\beta\leq\alpha}\begin{pmatrix}\alpha\\ \beta\end{pmatrix} D^{\alpha-\beta}\frac{1}{c(\boldsymbol{x})} D^\beta u\right| \\ &\leq C\omega^2 \sum_{\beta\leq\alpha} |D^\beta u|.\end{aligned}$$

This shows that

$$\left\|D^\alpha\left(\frac{\omega}{c(\boldsymbol{x})}\right)^2 u\right\|_{L^2(\Omega)} \leq C\omega^2 \|u\|_{H^{|\alpha|}(\Omega)} \leq C\omega^2 \|u\|_{H^{2+|\alpha|}(\Omega)}.$$

Hence, we have

$$\left\| \left(\frac{\omega}{c(\boldsymbol{x})} \right)^2 u \right\|_{H^{k-1}(\Omega)} \leq C\omega^2 \|u\|_{H^{k+1}(\Omega)}, \quad \left\| \left(\frac{\omega}{c(\boldsymbol{x})} \right)^2 u \right\|_{H^{k-2}(\Omega)} \leq C\omega^2 \|u\|_{H^k(\Omega)}.$$

Thus, by Sobolev interpolation theory we obtain the upper bound of operator L.

For the boundary operator B, using Lemma 2.2 we obtain

$$\begin{aligned} \|Bu\|_{L^2(\partial\Omega)} &= \left\| \frac{\partial u}{\partial \boldsymbol{n}} - i\frac{\omega}{c(\boldsymbol{x})} u \right\|_{L^2(\partial\Omega)} \\ &\leq \|\nabla u\|_{L^2(\partial\Omega)} + \frac{\omega}{c_{\min}} \|u\|_{L^2(\partial\Omega)} \\ &\leq C\frac{\omega}{c_{\min}} \|u\|_{H^1(\partial\Omega)}. \end{aligned}$$

This completes the proof. □

4 One-level RBF collocation

We want to use the trial spaces produced by radial basis functions as finite dimensional approximation of the Eqs. (3.2a)-(3.2b). In fact, such trial spaces are the subspaces of the reproducing kernel Hilbert spaces (or native spaces). The reproducing kernel plays an important role in our later analysis.

Definition 4.1. *Let H be a real Hilbert space of functions $f:\Omega(\subseteq\mathbb{R}^d)\to\mathbb{R}$ with inner product $\langle\cdot,\cdot\rangle_H$. A function $\Phi:\Omega\times\Omega\to\mathbb{R}$ is called reproducing kernel for H if*

(1). $\Phi(\cdot,\boldsymbol{x})\in H$ for all $\boldsymbol{x}\in\Omega$,

(2). $f(\boldsymbol{x})=\langle f,\Phi(\cdot,\boldsymbol{x})\rangle_H$ for all $f\in H$ and all $\boldsymbol{x}\in\Omega$.

A translation-invariant kernel such as the strictly positive definite radial function $\Phi(\boldsymbol{x},\boldsymbol{y})=\Phi(\boldsymbol{x}-\boldsymbol{y})$ will generate a reproducing kernel Hilbert space, the so-called native space $\mathcal{N}_\Phi(\Omega)$. But we will make use of the native space $\mathcal{N}_\Phi(\mathbb{R}^d)$ which defined in $\mathbb{R}^d$ and described by Fourier transform (2.1). $\mathcal{N}_\Phi(\mathbb{R}^d)$ consists of all functions $f\in L^2(\mathbb{R}^d)$ with

$$\|f\|_\Phi^2 = \int_{\mathbb{R}^d} \frac{|\widehat{f}(\boldsymbol{\omega})|^2}{\widehat{\Phi}(\boldsymbol{\omega})} d\boldsymbol{\omega} < \infty. \tag{4.1}$$

Hence, if the Fourier transform of $\Phi:\mathbb{R}^d\to\mathbb{R}$ has the algebraic decay condition

$$c_1(1+\|\boldsymbol{\omega}\|_2^2)^{-\sigma} \leq \widehat{\Phi}(\omega) \leq c_2(1+\|\boldsymbol{\omega}\|_2^2)^{-\sigma} \tag{4.2}$$

for two fixed constants $0<c_1<c_2$, then the native space $\mathcal{N}_\Phi(\mathbb{R}^d)$ will be norm equivalent to the Sobolev space $H^\sigma(\mathbb{R}^d)$. In the paper, we always use Φ to represent the radial

functions which satisfy the condition (4.2). Thus, with a radial function Φ satisfied (4.2) and a scaling parameter $\delta\in(0,1]$, we can construct a scaled radial function

$$\Phi_\delta := \delta^{-d}\Phi((\boldsymbol{x}-\boldsymbol{y})/\delta), \quad \boldsymbol{x},\boldsymbol{y}\in\mathbb{R}^d. \tag{4.3}$$

The following Lemma establishes a relation between the native space $\mathcal{N}_{\Phi_\delta}(\mathbb{R}^d)$ and the Sobolev space $H^\sigma(\mathbb{R}^d)$. Its proof can be found in [34].

Lemma 4.1 (Norm Equivalence)**.** *For every $\delta\in(0,1]$ we have $\mathcal{N}_{\Phi_\delta}(\mathbb{R}^d)=H^\sigma(\mathbb{R}^d)$. And we have for every $f\in H^\sigma(\mathbb{R}^d)$ the norm equivalence*

$$c_1\|f\|_{\Phi_\delta}\le\|f\|_{H^\sigma(\mathbb{R}^d)}\le c_2\delta^{-\sigma}\|f\|_{\Phi_\delta} \tag{4.4}$$

with $c_1,c_2>0$.

Let $X=\{\boldsymbol{x}_1,\boldsymbol{x}_2,\cdots,\boldsymbol{x}_{N_I},\boldsymbol{x}_{N_I+1},\cdots,\boldsymbol{x}_N\}\subset\overline{\Omega}$ be some scattered centers in $\mathbb{R}^d$, which include N_I interior points and $N-N_I$ boundary points. We denote the set of interior points and boundary points as X^I and X^B respectively. Then $X=X^I\bigcup X^B$, and X^I,X^B are nonempty sets. Let h_I denote the fill distance of the set X^I in Ω, which is usually defined as

$$h_I := \sup_{\boldsymbol{x}\in\Omega}\min_{\boldsymbol{x}_j\in X^I}\|\boldsymbol{x}-\boldsymbol{x}_j\|_2.$$

For the boundary points, we define the fill distance by using ψ_j and the partition of unity, that is

$$h_B := \max_{1\le j\le K}\left\{\sup_{\boldsymbol{x}\in B=B(\boldsymbol{0},1)}\min_{\boldsymbol{x}_j\in\psi_j^{-1}\left(X^B\cap V_j\right)}\|\boldsymbol{x}-\boldsymbol{x}_j\|_2\right\}.$$

Then, a symmetric collocation for (3.2a)-(3.2b) is finding a trial function with the form

$$s(\boldsymbol{x})=\sum_{j=1}^{N_I}c_jL^{\boldsymbol{y}}\Phi_\delta(\boldsymbol{x}-\boldsymbol{y})\Big|_{\boldsymbol{y}=\boldsymbol{x}_j}+\sum_{j=N_I+1}^{N}c_jB^{\boldsymbol{y}}\Phi_\delta(\boldsymbol{x}-\boldsymbol{y})\Big|_{\boldsymbol{y}=\boldsymbol{x}_j}, \quad \boldsymbol{x}_j\in X, \tag{4.5}$$

which satisfies

$$Ls(\boldsymbol{x}_i)=f(\boldsymbol{x}_i), \quad i=1,\cdots,N_I, \tag{4.6a}$$
$$Bs(\boldsymbol{x}_i)=g(\boldsymbol{x}_i), \quad i=N_I+1,\cdots,N. \tag{4.6b}$$

Here $L^{\boldsymbol{y}}$ and $B^{\boldsymbol{y}}$ are the differential operators used in (3.2a)-(3.2b), but acting on Φ viewed as a function of the second argument. The symmetric collocation (4.5) is based on the generalized Hermite interpolation method which is developed in [37]. In order to be able to apply the results from generalized Hermite interpolation that will ensure the non-singularity of the collocation matrix, [14] proposed the symmetric collocation. It differs from the non-symmetric collocation [20], where the specific format of $s(\boldsymbol{x})$ is written as

$$s(\boldsymbol{x})=\sum_{j=1}^{N}c_j\Phi_\delta(\boldsymbol{x}-\boldsymbol{x}_j), \quad \boldsymbol{x}_j\in X.$$

Compared with the symmetric collocation method, non-symmetric collocation method is more flexible and concise. It avoids constructing the trial space based on complicated differential operator or implementing the numerical integration. However, [19] shows that this method may be failure for some scattered data sites with the special distribution. It cannot be well-posed for arbitrary centers locations and may produce a singular collocation matrix. So it is now an open question to find sufficient conditions on the centers locations that guarantee invertibility of the non-symmetric collocation matrix. This is the reason why we use the symmetric collocation in the paper.

Then, the linear system (4.6a)-(4.6b) can produce a collocation matrix A that is of the form

$$A=\begin{pmatrix} A_{LL^y} & A_{LB^y} \\ A_{BL^y} & A_{BB^y} \end{pmatrix}. \tag{4.7}$$

Here the four blocks are generated as follows:

$$\begin{aligned}
&(A_{LL^y})_{ij}=LL^{\boldsymbol{y}}\Phi(\boldsymbol{x}-\boldsymbol{y})|_{\boldsymbol{x}=\boldsymbol{x}_i,\boldsymbol{y}=\boldsymbol{x}_j}, && \boldsymbol{x}_i\in X^I, && \boldsymbol{x}_j\in X^I,\\
&(A_{LB^y})_{ij}=LB^{\boldsymbol{y}}\Phi(\boldsymbol{x}-\boldsymbol{y})|_{\boldsymbol{x}=\boldsymbol{x}_i,\boldsymbol{y}=\boldsymbol{x}_j}, && \boldsymbol{x}_i\in X^I, && \boldsymbol{x}_j\in X^B,\\
&(A_{BL^y})_{ij}=BL^{\boldsymbol{y}}\Phi(\boldsymbol{x}-\boldsymbol{y})|_{\boldsymbol{x}=\boldsymbol{x}_i,\boldsymbol{y}=\boldsymbol{x}_j}, && \boldsymbol{x}_i\in X^B, && \boldsymbol{x}_j\in X^I,\\
&(A_{BB^y})_{ij}=BB^{\boldsymbol{y}}\Phi(\boldsymbol{x}-\boldsymbol{y})|_{\boldsymbol{x}=\boldsymbol{x}_i,\boldsymbol{y}=\boldsymbol{x}_j}, && \boldsymbol{x}_i\in X^B, && \boldsymbol{x}_j\in X^B.
\end{aligned}$$

The matrix A of (4.7) is of the same type as the generalized Hermite interpolation matrix, it is symmetric and therefore non-singular as long as Φ is chosen appropriately. So, viewed using the expansion (4.5) for $s(\boldsymbol{x})$, the symmetric collocation method is apparently well-posed.

We now want to bound the L^2 error between the solution u and its symmetric approximation s.

Theorem 4.1 (Convergence of one-level collocation). *Let $\sigma\in\mathbb{R}$, and $k=\lfloor\sigma\rfloor>d/2+2$. Let $\Omega\subset\mathbb{R}^d$ ($d=1,2,3$) be a bounded connected Lipschitz domain with $C^{k,s}-$boundary for $s\in[0,1)$. Let $c(\boldsymbol{x})\in W^{k-1,\infty}(\Omega)$. Suppose the solution of* (3.2a)-(3.2b) *has the regularity $u\in H^\sigma(\Omega)$. Assume that $\delta\in(0,1]$. Suppose s is the collocation solution that satisfies* (4.6a)-(4.6b). *Then there exists a constant $C>0$ such that*

$$\|u-s\|_{L^2(\Omega)}\le C\cdot C(\omega)\delta^{-\sigma}h^{\sigma-2}\|u\|_{H^\sigma(\Omega)},$$

where C is independent of ω, $c_{\min}$, $c_{\max}$, δ, h, and

$$h=\max\{h_I,h_B\},\quad C(\omega):=\sqrt{C_{stab}\cdot c_{\max}}\cdot\left[\omega^3+\frac{\omega}{c_{\min}^2}\right]^{1/2}.$$

Proof. With the help of the priori inequality (Theorem 3.2) we have

$$\|u-s\|^2_{L^2(\Omega)}\le C_{stab}\frac{c_{\max}}{\omega}\left(\|Lu-Ls\|^2_{L^2(\Omega)}+\|Bu-Bs\|^2_{L^2(\partial\Omega)}\right).$$

So we need to bound the two terms on the right-hand side separately.

By using the sampling inequality of [27], Lemmas 3.1, 2.1, 4.1, and Theorem 16.1 in [33], we have

$$\begin{aligned}\|Lu-Ls\|^2_{L^2(\Omega)} \leq & Ch_I^{2(\sigma-2)}\|Lu-Ls\|^2_{H^{\sigma-2}(\Omega)}\\ \leq & C\omega^4 h_I^{2(\sigma-2)}\|u-s\|^2_{H^\sigma(\Omega)}\\ \leq & C\omega^4 h_I^{2(\sigma-2)}\|Eu-s_E\|^2_{H^\sigma(\mathbb{R}^d)}\\ \leq & C\omega^4\delta^{-2\sigma}h_I^{2(\sigma-2)}\|Eu-s_E\|^2_{\Phi_\delta}\\ \leq & C\omega^4\delta^{-2\sigma}h_I^{2(\sigma-2)}\|Eu\|^2_{\Phi_\delta}.\end{aligned}$$

For the boundary term, by using Lemma 3.1, the sampling inequality, Lemma 2.3, and the proof process as for the above term, we have

$$\begin{aligned}\|Bu-Bs\|^2_{L^2(\partial\Omega)} \leq & C\left(\frac{\omega}{c_{\min}}\right)^2\|u-s\|^2_{H^1(\partial\Omega)} = C\left(\frac{\omega}{c_{\min}}\right)^2\sum_{j=1}^k\|v_j\|^2_{H^1(B)}\\ \leq & C\left(\frac{\omega}{c_{\min}}\right)^2\sum_{j=1}^k h_{T_j,B}^{2(\sigma-3/2)}\|v_j\|^2_{H^{\sigma-1/2}(B)}\\ \leq & C\left(\frac{\omega}{c_{\min}}\right)^2 h_B^{2(\sigma-3/2)}\|u-s\|^2_{H^{\sigma-1/2}(\partial\Omega)}\\ \leq & C\left(\frac{\omega}{c_{\min}}\right)^2 h_B^{2(\sigma-3/2)}\|u-s\|^2_{H^\sigma(\Omega)}\\ \leq & C\left(\frac{\omega}{c_{\min}}\right)^2\delta^{-2\sigma}h_B^{2(\sigma-3/2)}\|Eu\|^2_{\Phi_\delta}.\end{aligned}$$

Hence, by combining the above two results we can conclude

$$\begin{aligned}\|u-s\|^2_{L^2(\Omega)} \leq & C\cdot C_{stab}\frac{c_{\max}}{\omega}\delta^{-2\sigma}\left[\omega^4 h_I^{2(\sigma-2)}+\left(\frac{\omega}{c_{\min}}\right)^2 h_B^{2(\sigma-3/2)}\right]\|Eu\|^2_{\Phi_\delta}\\ \leq & C\cdot C_{stab}\frac{c_{\max}}{\omega}\left[\omega^4+\left(\frac{\omega}{c_{\min}}\right)^2\right]\delta^{-2\sigma}h^{2(\sigma-2)}\|Eu\|^2_{\Phi_\delta}\\ \leq & C\cdot C_{stab}\frac{c_{\max}}{\omega}\left[\omega^4+\left(\frac{\omega}{c_{\min}}\right)^2\right]\delta^{-2\sigma}h^{2(\sigma-2)}\|Eu\|^2_{H^\sigma(\mathbb{R}^d)}\\ \leq & C\cdot C_{stab}\frac{c_{\max}}{\omega}\left[\omega^4+\left(\frac{\omega}{c_{\min}}\right)^2\right]\delta^{-2\sigma}h^{2(\sigma-2)}\|u\|^2_{H^\sigma(\Omega)}.\end{aligned}$$

This completes the proof. □

5 Multilevel RBF collocation

We now consider implementing the symmetric collocation for (3.2a)-(3.2b) on the increasingly dense data sites. Assume that we are given a sequence of interior centers $X_1^I, X_2^I, \cdots \subset \Omega$ with fill distance $h_{X_1^I}, h_{X_2^I}, \cdots$, and boundary centers $X_1^B, X_2^B, \cdots \subset \partial\Omega$ with fill distance $h_{X_1^B}, h_{X_2^B}, \cdots$. We denote

$$h_j = \max\{h_{X_j^I}, h_{X_j^B}\}, \quad X_j = X_j^I \bigcup X_j^B \subset \overline{\Omega}.$$

With a radial function Φ satisfied (4.2) and a series of decreasing scaling parameters $\delta_1 > \delta_2 > \cdots > \delta_j > \cdots \in (0,1]$, we can define

$$\Phi_j := \Phi_{\delta_j} = \delta_j^{-d} \Phi((\boldsymbol{x}-\boldsymbol{y})/\delta_j), \quad \boldsymbol{x},\boldsymbol{y} \in \mathbb{R}^d. \tag{5.1}$$

Using the radial functions Φ_j and the trial centers X_j, the one-level kernel-based trial spaces can be constructed as

$$W_j = \text{span}\{L^{\boldsymbol{y}} \Phi_j(\cdot - \boldsymbol{y})|_{\boldsymbol{y}=\boldsymbol{x}_j},\ \boldsymbol{x}_j \in X_j^I\} \bigcup \text{span}\{B^{\boldsymbol{y}} \Phi_j(\cdot - \boldsymbol{y})|_{\boldsymbol{y}=\boldsymbol{x}_j},\ \boldsymbol{x}_j \in X_j^B\}. \tag{5.2}$$

Then a multilevel collocation algorithm for the Eqs. (3.2a)-(3.2b) can be obtained as the following form.

Algorithm 5.1 (Multilevel collocation)**.** Given the right-hand sides f and g, we implement

(1). Set $u_0 = 0$, $f_0 = f$, $g_0 = g$

(2). for $j = 1,2,\cdots$, do

• Determine the local collocation $s_j \in W_j$ to f_{j-1} and g_{j-1} with

$$Ls_j(\boldsymbol{x}) = f_{j-1}(\boldsymbol{x}), \quad \boldsymbol{x} \in X_j^I, \tag{5.3a}$$

$$Bs_j(\boldsymbol{x}) = g_{j-1}(\boldsymbol{x}), \quad \boldsymbol{x} \in X_j^B, \tag{5.3b}$$

• Update the global approximation and the residuals

$$u_j = u_{j-1} + s_j, \quad f_j = f_{j-1} - Ls_j, \quad g_j = g_{j-1} - Bs_j.$$

The multilevel collocation has been used for various scientific and engineering calculations successfully [6–9, 12, 13, 15, 23, 32, 35, 36]. We are now ready to prove the L^2 error of multilevel symmetric collocation for the Eqs. (3.2a)-(3.2b). The proof is very similar to the technical process of [7, 12, 34], and [36].

Theorem 5.1 (Convergence of multilevel collocation). *Let $\sigma\in\mathbb{R}$, and $k=\lfloor\sigma\rfloor>d/2+2$. Let $\Omega\subset\mathbb{R}^d$ ($d=1,2,3$) be a bounded connected Lipschitz domain with $C^{k,s}-$boundary for $s\in[0,1)$. Let $c(\boldsymbol{x})\in W^{k-1,\infty}(\Omega)$. Suppose the solution of* (3.2a)-(3.2b) *has the regularity $u\in H^\sigma(\Omega)$. Suppose $s_j\in W_j$ are the local collocation decided by Algorithm* 5.1. *Assume that δ_j, h_j satisfy the relations:*

$$\delta_j=\left(\frac{h_j}{\mu}\right)^{1-2/\sigma},\quad h_j=\mu h_{j-1},\quad j=1,2,\cdots, \tag{5.4}$$

with appropriate h_0 and $0<\mu<1$. And assume the constant μ has been chosen sufficiently small such that

$$\alpha:=C\cdot C(\omega)\mu^{\sigma-2}<1.$$

Then there exists a constant $C>0$ such that

$$\|u-u_k\|_{L^2(\Omega)}\le C\cdot C(\omega)\alpha^k\|u\|_{H^\sigma(\Omega)}.$$

Proof. Let $e_j=u-u_j$, then

$$e_j=u-\sum_{k=1}^{j}s_k=e_{j-1}-s_j.$$

We now consider the relationship between e_j and e_{j-1} under the action of Sobolev extension operator E. By using the definition of the native space $\mathcal{N}_{\Phi_{j+1}}(\mathbb{R}^d)$, we have

$$\begin{aligned}
\|Ee_j\|^2_{\Phi_{j+1}}&=\int_{\mathbb{R}^d}\frac{|\widehat{Ee_j}(\boldsymbol{\omega})|^2}{\widehat{\Phi_{j+1}}(\boldsymbol{\omega})}d\boldsymbol{\omega}=\int_{\mathbb{R}^d}\frac{|\widehat{Ee_j}(\boldsymbol{\omega})|^2}{\widehat{\Phi}(\delta_{j+1}\boldsymbol{\omega})}d\boldsymbol{\omega}\\
&\le C\int_{\mathbb{R}^d}|\widehat{Ee_j}(\boldsymbol{\omega})|^2(1+\delta_{j+1}^2\|\boldsymbol{\omega}\|_2^2)^\sigma d\boldsymbol{\omega}\\
&\le C\int_{\|\boldsymbol{\omega}\|_2\le\frac{1}{\delta_{j+1}}}|\widehat{Ee_j}(\boldsymbol{\omega})|^2(1+\delta_{j+1}^2\|\boldsymbol{\omega}\|_2^2)^\sigma d\boldsymbol{\omega}\\
&\quad+C\int_{\|\boldsymbol{\omega}\|_2\ge\frac{1}{\delta_{j+1}}}|\widehat{Ee_j}(\boldsymbol{\omega})|^2(1+\delta_{j+1}^2\|\boldsymbol{\omega}\|_2^2)^\sigma d\boldsymbol{\omega}=:CI_1+CI_2.
\end{aligned}$$

For the first term I_1, using Lemma 2.1, the one-level convergence result (Theorem 4.1), and Lemma 4.1 leads to

$$\begin{aligned}
I_1&\le 2^\sigma\int_{\|\boldsymbol{\omega}\|_2\le\frac{1}{\delta_{j+1}}}|\widehat{Ee_j}(\boldsymbol{\omega})|^2d\boldsymbol{\omega}\\
&\le 2^\sigma\int_{\mathbb{R}^d}|\widehat{Ee_j}(\boldsymbol{\omega})|^2d\boldsymbol{\omega}\\
&=2^\sigma\|Ee_j\|^2_{L^2(\mathbb{R}^d)}\le C\|e_j\|^2_{L^2(\Omega)}\\
&\le C\cdot C^2(\omega)\delta_j^{-2\sigma}h_j^{2(\sigma-2)}\|Ee_{j-1}\|^2_{\Phi_j}\\
&\le C\cdot C^2(\omega)\mu^{2(\sigma-2)}\|Ee_{j-1}\|^2_{\Phi_j}.
\end{aligned}$$

For the second term on the right-hand side, we use the norm definition of $H^\sigma(\mathbb{R}^d)$, Lemmas 2.1, and 4.1 to obtain

$$\begin{aligned}
I_2 \leq & 2^\sigma \delta_{j+1}^{2\sigma} \int_{\|\boldsymbol{\omega}\|_2 \geq \frac{1}{\delta_{j+1}}} |\widehat{Ee_j}(\boldsymbol{\omega})|^2 \|\boldsymbol{\omega}\|_2^{2\sigma} d\boldsymbol{\omega} \\
\leq & 2^\sigma \delta_{j+1}^{2\sigma} \int_{\mathbb{R}^d} |\widehat{Ee_j}(\boldsymbol{\omega})|^2 (1+\|\boldsymbol{\omega}\|_2^2)^\sigma d\boldsymbol{\omega} \\
\leq & 2^\sigma \delta_{j+1}^{2\sigma} \|Ee_j\|_{H^\sigma(\mathbb{R}^d)}^2 \leq C\delta_{j+1}^{2\sigma} \|e_j\|_{H^\sigma(\Omega)}^2 \\
= & C\delta_{j+1}^{2\sigma} \|Ee_{j-1} - s_{Ee_{j-1}}\|_{H^\sigma(\Omega)}^2 \\
\leq & C\delta_{j+1}^{2\sigma} \|Ee_{j-1} - s_{Ee_{j-1}}\|_{H^\sigma(\mathbb{R}^d)}^2 \\
\leq & C\delta_{j+1}^{2\sigma} \delta_j^{-2\sigma} \|Ee_{j-1} - s_{Ee_{j-1}}\|_{\Phi_j}^2 \\
\leq & C\mu^{2(\sigma-2)} \|Ee_{j-1}\|_{\Phi_j}^2.
\end{aligned}$$

From the upper bounds of I_1, I_2, choosing $\alpha = C \cdot C(\omega)\mu^{\sigma-2}$, we have

$$\|Ee_j\|_{\Phi_{j+1}} \leq C \cdot C(\omega)\mu^{\sigma-2} \|Ee_{j-1}\|_{\Phi_j} = \alpha \|Ee_{j-1}\|_{\Phi_j}. \tag{5.5}$$

Then we obtain

$$\begin{aligned}
\|u - u_k\|_{L^2(\Omega)} = & \|e_k\|_{L^2(\Omega)} \\
\leq & C \cdot C(\omega) h_k^{\sigma-2} \|Ee_k\|_{H^\sigma(\mathbb{R}^d)} \\
\leq & C \cdot C(\omega) h_k^{\sigma-2} \delta_{k+1}^{-\sigma} \|Ee_k\|_{\Phi_{k+1}} \\
\leq & C \cdot C(\omega) \|Ee_k\|_{\Phi_{k+1}}.
\end{aligned}$$

Then using (5.5) k times, we have

$$\|u - u_k\|_{L^2(\Omega)} \leq C \cdot C(\omega) \|Ee_k\|_{\Phi_{k+1}} \leq \cdots \leq C \cdot C(\omega)\alpha^k \|Eu\|_{\Phi_1} \leq C \cdot C(\omega)\alpha^k \|u\|_{H^\sigma(\Omega)}.$$

This completes the proof. □

6 Numerical examples

We restrict ourselves here to the two-dimensional numerical experiments. We denote $\boldsymbol{x} = (x, y)$, $\boldsymbol{\xi} = (\xi, \eta) \in \Omega \subseteq \mathbb{R}^2$. Given one of the radial basis functions

$$\Phi(\boldsymbol{x} - \boldsymbol{\xi}) = \Phi\Big(\sqrt{(x-\xi)^2 + (y-\eta)^2}\Big),$$

we can derive the expression after the differential operators are applied:

$$
\begin{aligned}
LL^{\xi}\Phi &= \Delta^2\Phi+\left(\frac{\omega}{c(\xi,\eta)}\right)^2\Delta\Phi+\left(\frac{\omega}{c(x,y)}\right)^2\Delta\Phi+\left(\frac{\omega}{c(x,y)}\right)^2\left(\frac{\omega}{c(\xi,\eta)}\right)^2\Phi,\\
LB^{\xi}\Phi &= -n_1(\xi,\eta)\Delta\Phi_{\xi}-n_2(\xi,\eta)\Delta\Phi_{\eta}+i\frac{\omega}{c(\xi,\eta)}\Delta\Phi-\left(\frac{\omega}{c(x,y)}\right)^2 n_1(\xi,\eta)\Phi_{\xi}\\
&\quad-\left(\frac{\omega}{c(x,y)}\right)^2 n_2(\xi,\eta)\Phi_{\eta}+i\left(\frac{\omega}{c(x,y)}\right)^2\frac{\omega}{c(\xi,\eta)}\Phi,\\
BL^{\xi}\Phi &= -n_1(x,y)\Delta\Phi_{x}-n_2(x,y)\Delta\Phi_{y}+i\frac{\omega}{c(x,y)}\Delta\Phi-\left(\frac{\omega}{c(\xi,\eta)}\right)^2 n_1(x,y)\Phi_{x}\\
&\quad-\left(\frac{\omega}{c(\xi,\eta)}\right)^2 n_2(x,y)\Phi_{y}+i\left(\frac{\omega}{c(\xi,\eta)}\right)^2\frac{\omega}{c(x,y)}\Phi,\\
BB^{\xi}\Phi &= n_1(x,y)n_1(\xi,\eta)\Phi_{\xi x}+n_1(x,y)n_2(\xi,\eta)\Phi_{\eta x}-in_1(x,y)\frac{\omega}{c(\xi,\eta)}\Phi_x\\
&\quad+n_2(x,y)n_1(\xi,\eta)\Phi_{\xi y}+n_2(x,y)n_2(\xi,\eta)\Phi_{\eta y}-in_2(x,y)\frac{\omega}{c(\xi,\eta)}\Phi_y\\
&\quad-i\frac{\omega}{c(x,y)}n_1(\xi,\eta)\Phi_{\xi}-i\frac{\omega}{c(x,y)}n_2(\xi,\eta)\Phi_{\eta}-\frac{\omega}{c(x,y)}\frac{\omega}{c(\xi,\eta)}\Phi,
\end{aligned}
$$

147 here $\boldsymbol{n}=(n_1,n_2)$ is the outward unit normal vector on $\partial\Omega$.

Since we consider complex operators, we also need to conjugate the operators in order to get a Hermitian matrix in the end. Denote $\bar{B}^{\xi}$ as the conjugate of B^{ξ}. If we replace B^{ξ} by $\bar{B}^{\xi}$ in the above derivation, we will get a Hermitian matrix which will be more convenient for numerical calculation. In addition, because $\Delta^{\xi}\Phi=\Delta\Phi$, $\Phi_x=-\Phi_{\xi}$, and $\Phi_y=-\Phi_{\eta}$, so we only need to consider the action of differential operators on variables $\boldsymbol{x}=(x,y)$. In the following experiments, we use Wendland's C^6 radial basis function

$$\Phi(\boldsymbol{x},\boldsymbol{\xi})=[(1-\varepsilon r)_+]^8(32(\varepsilon r)^3+25(\varepsilon r)^2+8\varepsilon r+1)\quad\text{with}\quad r=\sqrt{(x-\xi)^2+(y-\eta)^2}$$

and a scaling parameter $\varepsilon:=1/\delta>0$. Then,

$$
\begin{aligned}
&\Phi_x=-22\varepsilon^2 x[16(\varepsilon r)^2+7\varepsilon r+1][(1-\varepsilon r)_+]^7,\quad \Phi_y=-22\varepsilon^2 y[16(\varepsilon r)^2+7\varepsilon r+1][(1-\varepsilon r)_+]^7,\\
&\Phi_{xx}=22\varepsilon^2\frac{1}{r^2}\left[x^2(160(\varepsilon r)^3+15(\varepsilon r)^2-6\varepsilon r-1)+y^2(16(\varepsilon r)^3-9(\varepsilon r)^2-6\varepsilon r-1)\right][(1-\varepsilon r)]_+^6,\\
&\Phi_{yy}=22\varepsilon^2\frac{1}{r^2}\left[y^2(160(\varepsilon r)^3+15(\varepsilon r)^2-6\varepsilon r-1)+x^2(16(\varepsilon r)^3-9(\varepsilon r)^2-6\varepsilon r-1)\right][(1-\varepsilon r)_+]^6,\\
&\Phi_{xy}=528\varepsilon^4 xy(6\varepsilon r+1)[(1-\varepsilon r)_+]^6,\quad \Delta\Phi=44\varepsilon^2[88(\varepsilon r)^3+3(\varepsilon r)^2-6\varepsilon r-1][(1-\varepsilon r)_+]^6,\\
&\Delta\Phi_x=-1056\varepsilon^4 x[33(\varepsilon r)^2-10\varepsilon r-2][(1-\varepsilon r)_+]^5,\\
&\Delta\Phi_y=-1056\varepsilon^4 y[33(\varepsilon r)^2-10\varepsilon r-2][(1-\varepsilon r)_+]^5,\\
&\Delta^2\Phi=1056\varepsilon^4[297(\varepsilon r)^3-212(\varepsilon r)^2+16\varepsilon r+4][(1-\varepsilon r)_+]^4.
\end{aligned}
$$

In our numerical experiments, the computations were performed on a laptop with 2.2 GHz Intel Core i7-1360P processor, using MATLAB running in the Windows 11 operating system. The discrete linear system is solved by a MATLAB operator "\".

6.1 Example 1 (regular domain)

We first consider the one-level and multilevel collocation methods for (3.2a)-(3.2b) on a square domain $\Omega=[0,1]^2$. We choose the exact solution and the variable wave speed as

$$u(x,y)=\sin(\pi x)\sin(\pi y)e^{-i\omega(x+y)},\quad c(x,y)=\left(\sqrt{\frac{1}{2}\sin\left(2\pi\sqrt{x^2+y^2}\right)+5}\right)^{-1},$$

and the source term as

$$\begin{aligned}f(x,y)=&2(\pi^2+\omega^2)\sin(\pi x)\sin(\pi y)e^{-i\omega(x+y)}+2i\omega\pi(\cos(\pi x)\sin(\pi y)\\&+\cos(\pi y)\sin(\pi x))e^{-i\omega(x+y)}\\&-\omega^2(0.5\sin(2\pi\sqrt{x^2+y^2})+5)\sin(\pi x)\sin(\pi y)e^{-i\omega(x+y)}.\end{aligned}$$

We know that Wendland's C^6 radial basis function can generate Sobolev space $H^\sigma(\mathbb{R}^2)$ with $\sigma=4.5$. Simple calculation shows that the convergence order of one-level collocation method is, approximately, 2.5. We choose the point sets to be on nested uniform grids and create additional equally spaced $4(h^{-1/2}-1)$ boundary points. For the one-level collocation case, we fix $\delta=2.0$. Table 1 shows the L^2 error and convergence rate of one-level collocation. From Table 1, we observe that the rate is consistent with the results of the Theorem 4.1 when ω is relatively small. But when $\omega=20$, the convergence rate is lower than 2.5 because the counteracting term $C(\omega)$ is affecting the convergence order. Fig. 1 gives the fill plots of the numerical solution for different frequencies. It shows that the simulation effect of the numerical solution is very consistent with the exact solution.

Table 1: Numerical results of one-level collocation method on square domain, when $\omega=1,10,20$.

h	$\omega=1$		$\omega=10$		$\omega=20$	
	L^2-error	rate	L^2-error	rate	L^2-error	rate
1/4	1.150410e-01	-	4.080607e-01	-	5.663582e-01	-
1/8	2.073224e-02	2.4722	6.446011e-02	2.6623	2.192027e-01	1.3694
1/16	2.871389e-03	2.8521	1.522878e-02	2.0816	1.535179e-02	3.8358
1/32	3.219845e-04	3.1567	3.230740e-03	2.2369	4.867683e-03	1.6571
1/64	3.189464e-05	3.3356	4.307717e-04	2.9069	1.483474e-03	1.7143

For the multilevel case, by using the conditions of the Theorem 5.1 we use a variable

$$\delta_j=v\left(\frac{h_j}{\mu}\right)^{1-2/\sigma},$$

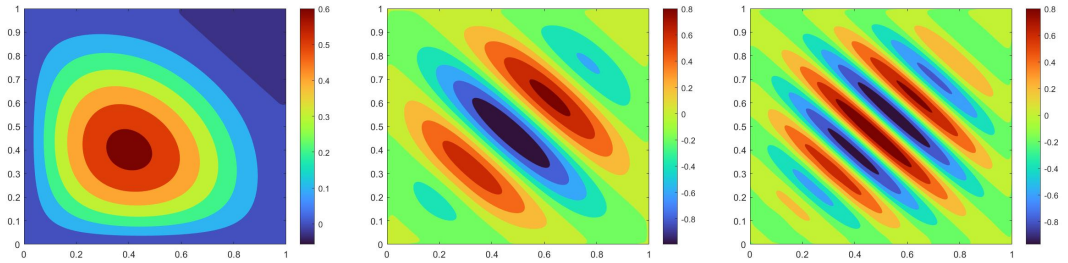

(a) $\omega=1$ (b) $\omega=10$ (c) $\omega=20$

Figure 1: The real part of the one-level numerical solution for different frequencies, when $h=1/32$ on square domain.

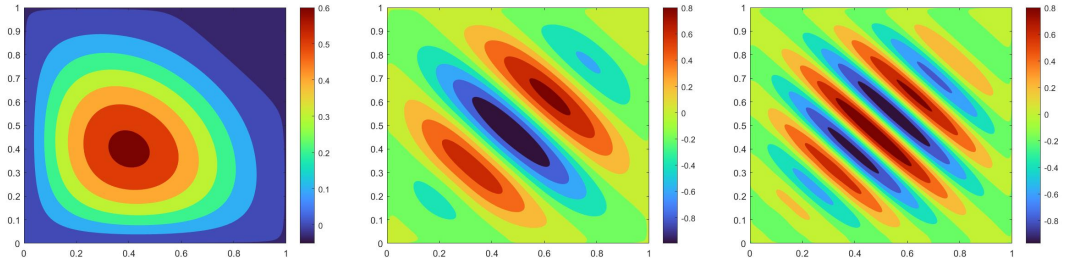

(a) $\omega=1$ (b) $\omega=10$ (c) $\omega=20$

Figure 2: The real part of the multilevel numerical solution for different frequencies, when $h=1/32$ on square domain.

with $\mu=1/2$. In order to be consistent with the experiments in [12], we select $v=2.4$. Table 2 shows the change process of δ, the L^2 error and convergence rate of multilevel collocation. From Table 2, we can see that the convergence rate is lower than the one-level case. This is due to the fact that the convergence order of the multilevel collocation is about $(2h)^{2.5}$ instead of $h^{2.5}$. However, by using multilevel method, the discrete matrix has better sparsity and condition number, thus speeding up the solution process. Fig. 2 gives the fill plots of the numerical solution for different frequencies. It shows that the modelling problem is still well simulated.

6.2 Example 2 (star domain)

We now consider an example is defined on an irregular domain. The boundary of this irregular domain is defined by the parameter equations:

$$\partial\Omega=\{(x,y)|x=\rho(\theta)\cos(\theta)+0.5,\ y=\rho(\theta)\sin(\theta)+0.5,\ 0\leq\theta\leq 2\pi\}$$

with

$$\rho(\theta)=\frac{0.9+0.1\sin(5\theta)}{2}.$$

Table 2: Numerical results of multilevel collocation method on square domain, when $\omega=1,10,20$.

δ	h	$\omega=1$		$\omega=10$		$\omega=20$	
		L^2-error	rate	L^2-error	rate	L^2-error	rate
1.6329	1/4	1.574715e-01	-	4.035495e-01	-	5.656354e-01	-
1.1111	1/8	7.404363e-02	1.0886	6.556042e-02	2.6218	2.172251e-01	1.3807
0.7560	1/16	2.951978e-02	1.3267	1.715437e-02	1.9342	1.581026e-02	3.7803
0.5144	1/32	9.557896e-03	1.6269	4.825416e-03	1.8299	5.074368e-03	1.6396
0.3500	1/64	2.478405e-03	1.9473	1.025810e-03	2.2339	1.781843e-03	1.5099

Table 3: Numerical results of one-level collocation method on star domain, when $\omega=1,10,20$.

h	$\omega=1$		$\omega=10$		$\omega=20$	
	L^2-error	rate	L^2-error	rate	L^2-error	rate
1/4	3.592399e-02	-	5.164890e-03	-	3.370509e-02	-
1/8	2.061473e-03	4.1232	6.333039e-04	3.0278	1.699101e-04	7.6321
1/16	1.935131e-04	3.4132	5.444790e-05	3.5399	1.179411e-05	3.8486
1/32	1.459235e-05	3.7291	6.809399e-06	2.9993	2.600095e-06	2.1814
1/64	1.198619e-06	3.6058	5.487727e-07	3.6332	3.278490e-07	2.9875

And the outward unit normal vector of $\partial\Omega$ is

$$n_1=\frac{n_x}{\sqrt{n_x^2+n_y^2}},\quad n_2=\frac{n_y}{\sqrt{n_x^2+n_y^2}},$$

here

$$\begin{aligned}n_x&=0.25\cos(5\theta)\sin(\theta)+0.5[0.9+0.1\sin(5\theta)]\cos(\theta),\\ n_y&=-0.25\cos(5\theta)\cos(\theta)+0.5[0.9+0.1\sin(5\theta)]\sin(\theta).\end{aligned}$$

We choose the exact solution and the variable wave speed as

$$u(x,y)=e^{-\omega\left((x-0.5)^2+(y-0.5)^2\right)},\quad c(x,y)=e^{-0.1\sin\left(\sqrt{x^2+y^2}\right)-0.5},$$

and the source term as

$$f(x,y)=\left(4\omega-4\omega^2((x-0.5)^2+(y-0.5)^2)-\omega^2e^{0.2\sin\left(\sqrt{x^2+y^2}\right)+1}\right)e^{-\omega\left((x-0.5)^2+(y-0.5)^2\right)}.$$

Although it is difficult to compare the convergence order on an irregular domain, we still provide the L^2 error and convergence rate of one-level collocation and multilevel collocation in Tables 3-4, respectively. It seems that the rate is little bit higher than the case of Example 1. Figs. 3-4 show the fill plots of the numerical solutions for different frequencies. We can observe that they are very consistent with the exact solution.

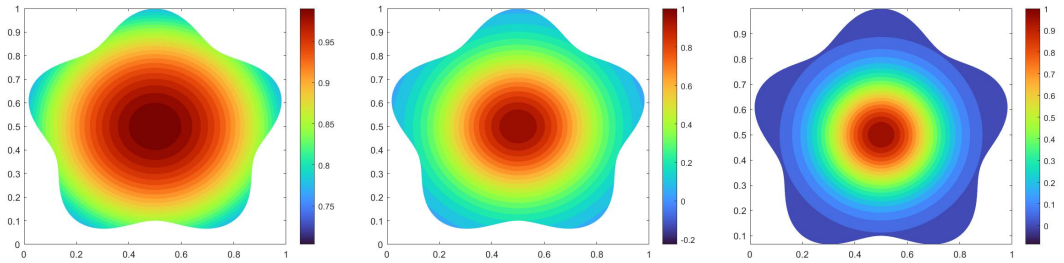

(a) $\omega=1$ (b) $\omega=10$ (c) $\omega=20$

Figure 3: The real part of the one-level numerical solution for different frequencies, when $h=1/32$ on star domain.

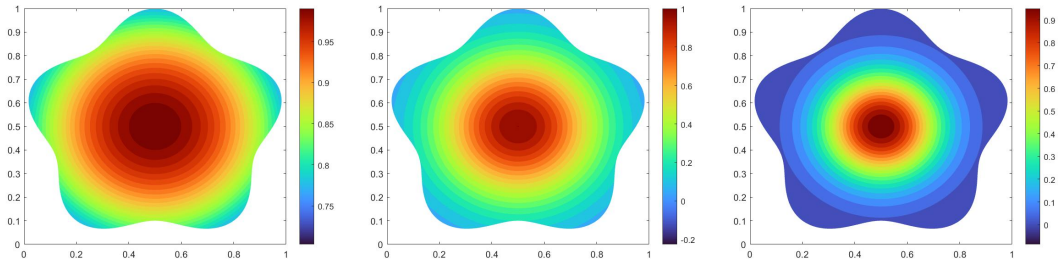

(a) $\omega=1$ (b) $\omega=10$ (c) $\omega=20$

Figure 4: The real part of the multilevel numerical solution for different frequencies, when $h=1/32$ on star domain.

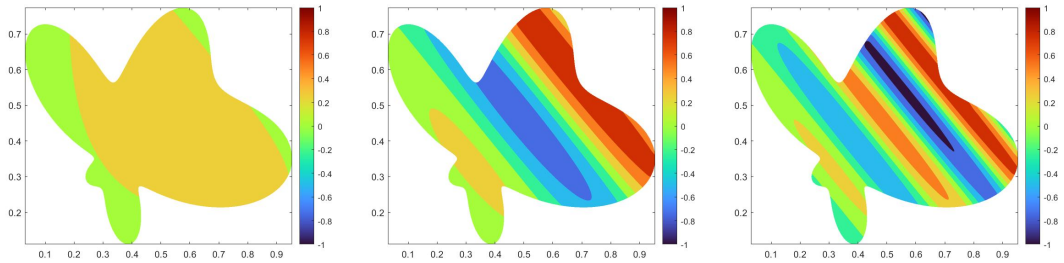

(a) $\omega=1$ (b) $\omega=10$ (c) $\omega=20$

Figure 5: The real part of the one-level numerical solution for different frequencies, when $N=1089$ on butterfly domain.

6.3 Example 3 (butterfly domain)

This example considers a butterfly domain. The butterfly interface defined by the parameter equation:

$$\partial\Omega=\{(x,y)|x=\rho(\theta)\cos(\theta)+0.35,\ y=\rho(\theta)\sin(\theta)+0.35,\ 0\leq\theta\leq 2\pi\},$$

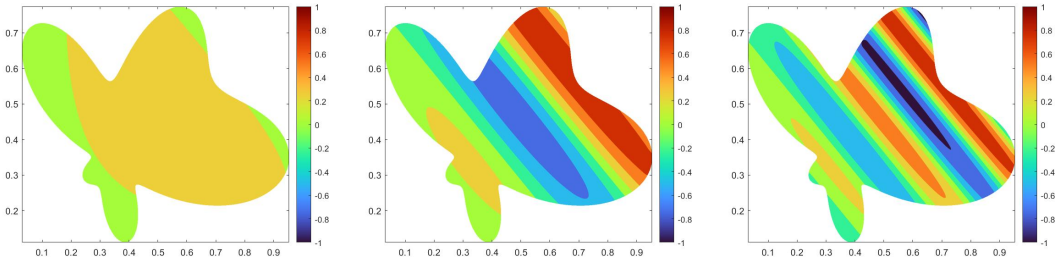

(a) $\omega=1$ (b) $\omega=10$ (c) $\omega=20$

Figure 6: The real part of the multilevel numerical solution for different frequencies, when $N=1089$ on butterfly domain.

with

$$\rho(\theta)=(e^{\sin(\theta)}\sin^2(2\theta)+e^{\cos(\theta)}\cos^2(2\theta))/4.5.$$

And the outward unit normal vector of $\partial\Omega$ is

$$n_1=\frac{n_x}{n_x^2+n_y^2},\quad n_2=\frac{n_y}{n_x^2+n_y^2},$$

here

$$\begin{aligned}n_x=&\frac{\sin(\theta)}{4.5}\left[e^{\sin(\theta)}\cos(\theta)\sin^2(2\theta)+2\sin(4\theta)e^{\sin(\theta)}-e^{\cos(\theta)}\sin(\theta)\cos^2(2\theta)\right.\\&\left.-2\sin(4\theta)e^{\cos(\theta)}\right]+\frac{\cos(\theta)}{4.5}\left[e^{\sin(\theta)}\sin^2(2\theta)+e^{\cos(\theta)}\cos^2(2\theta)\right],\\n_y=&-\frac{\cos(\theta)}{4.5}\left[e^{\sin(\theta)}\cos(\theta)\sin^2(2\theta)+2\sin(4\theta)e^{\sin(\theta)}-e^{\cos(\theta)}\sin(\theta)\cos^2(2\theta)\right.\\&\left.-2\sin(4\theta)e^{\cos(\theta)}\right]+\frac{\sin(\theta)}{4.5}\left[e^{\sin(\theta)}\sin^2(2\theta)+e^{\cos(\theta)}\cos^2(2\theta)\right].\end{aligned}$$

We choose the exact solution and the variable wave speed as

$$u(x,y)=\sin(\pi xy)e^{-i\omega(x+y)},\quad c(x,y)=1+0.5\sin(2\pi x),$$

and the source term as

$$\begin{aligned}f=&\pi^2(x^2+y^2)\sin(\pi xy)e^{-i\omega(x+y)}+2i\omega\pi(x+y)\cos(\pi xy)e^{-i\omega(x+y)}\\&+2\omega^2\sin(\pi xy)e^{-i\omega(x+y)}-\omega^2(1+0.5\sin(2\pi x))^{-2}\sin(\pi xy)e^{-i\omega(x+y)}.\end{aligned}$$

In this experiment, we choose $N=25,81,289,1089,4225$ Halton data sites which are randomly distributed in the interior domain. But on the boundary $\partial\Omega$, we arrange $4(\sqrt{N}-1)$ equidistant points according to polar angles. Tables 5-6 provide the L^2 error and convergence rate of one-level collocation and multilevel collocation respectively. We find that

Table 4: Numerical results of multilevel collocation method on star domain, when $\omega=1,10,20$.

δ	h	$\omega=1$		$\omega=10$		$\omega=20$	
		L^2-error	rate	L^2-error	rate	L^2-error	rate
1.6329	1/4	4.070963e-02	-	3.437267e-03	-	2.712704e-02	-
1.1111	1/8	6.623436e-03	2.6197	8.212335e-04	2.0654	5.951840e-04	5.5103
0.7560	1/16	1.368363e-03	2.2751	1.200983e-04	2.7736	1.630609e-04	1.8679
0.5144	1/32	2.219571e-04	2.6241	3.397697e-05	1.8216	5.068991e-05	1.6856
0.3500	1/64	3.402616e-05	2.7056	5.883681e-06	2.5298	1.026783e-05	2.3036

Table 5: Numerical results of one-level collocation method on butterfly domain, when $\omega=1,10,20$.

N	$\omega=1$		$\omega=10$		$\omega=20$	
	L^2-error	rate	L^2-error	rate	L^2-error	rate
25	1.504504e-02	-	1.759899e-01	-	8.819989e-01	-
81	3.454404e-04	5.4447	1.551704e-02	3.5036	1.397931e-01	2.6575
289	9.178573e-05	1.9121	8.413235e-04	4.2050	1.726511e-02	3.0174
1089	6.020187e-06	3.9304	7.618799e-05	3.4650	9.877943e-04	4.1275
4225	1.776984e-07	5.0823	6.210688e-06	3.6167	7.968292e-05	3.6319

Table 6: Numerical results of multilevel collocation method on butterfly domain, when $\omega=1,10,20$.

δ	N	$\omega=1$		$\omega=10$		$\omega=20$	
		L^2-error	rate	L^2-error	rate	L^2-error	rate
1.6329	25	1.893869e-02	-	1.708972e-01	-	8.783269e-01	-
1.1111	81	5.465632e-04	5.1148	1.757426e-02	3.2816	1.435739e-01	2.6130
0.7560	289	1.954274e-04	1.4838	1.089144e-03	4.0122	1.696510e-02	3.0812
0.5144	1089	2.130116e-05	3.1976	1.228255e-04	3.1485	1.158617e-03	3.8721
0.3500	4225	1.552557e-06	3.7782	1.723295e-05	2.8334	1.395661e-04	3.0534

the convergence rate is still quite higher even for the complex domain like the butterfly shape. Figs. 5-6 show the fill plots of the numerical solutions for different frequencies. We can still see that even for relatively large frequencies ω, the exact solution is still able to be approximated well.

6.4 Example 4 (M-shaped duct)

This example considers the wave propagation in an M-shaped duct. The upper and lower boundaries of the M-shaped duct can be defined by

$$y=0.3e^{-20(x-0.5)^2},\quad y=0.8-0.3\left(e^{-80(x-0.3)^2}+e^{-80(x-0.7)^2}\right).$$

We choose the exact solution and the variable wave speed as

$$u(x,y)=\frac{e^{-i\omega(x+y)}\sqrt{x^2+y^2}}{10},\quad c(x,y)=1+\sin(\pi x),$$

Table 7: Numerical results of one-level collocation method on M-shaped duct, when ω= 1, 10, 20.

N	$\omega=1$		$\omega=10$		$\omega=20$	
	L^2-error	rate	L^2-error	rate	L^2-error	rate
25	1.202931e-02	-	1.369322e-01	-	4.680121e-01	-
81	4.121063e-03	1.8225	1.059125e-02	4.3544	1.796101e-01	1.6293
289	1.749722e-03	1.3470	1.458086e-03	3.1178	1.673438e-02	3.7317
1089	8.703604e-04	1.0528	2.086351e-04	2.9313	1.988324e-03	3.2115
4225	2.086614e-04	2.1069	3.490594e-05	2.6375	1.802480e-04	3.5415

Table 8: Numerical results of multilevel collocation method on M-shaped duct, when $\omega=1,10,20$.

δ	N	$\omega=1$		$\omega=10$		$\omega=20$	
		L^2-error	rate	L^2-error	rate	L^2-error	rate
1.6329	25	2.949475e-02	-	1.317722e-01	-	4.566828e-01	-
1.1111	81	1.620794e-02	1.0186	1.259406e-02	3.9944	1.742291e-01	1.6394
0.7560	289	6.543452e-03	1.4262	3.160256e-03	2.1739	1.940484e-02	3.4511
0.5144	1089	2.689467e-03	1.3405	5.590315e-04	2.6115	2.283010e-03	3.2264
0.3500	4225	9.329308e-04	1.5619	1.438175e-04	2.0028	5.836243e-04	2.0121

and the source term is

$$f(x,y)=\left(\frac{\omega^2 e^{-i\omega(x+y)}\sqrt{x^2+y^2}}{5}+i\omega\frac{x+y}{5\sqrt{x^2+y^2}}e^{-i\omega(x+y)}-\frac{e^{-i\omega(x+y)}}{10\sqrt{x^2+y^2}}\right)$$
$$-\frac{\omega^2 e^{-i\omega(x+y)}\sqrt{x^2+y^2}}{10(1+\sin(\pi x))^2}.$$

Compared with the previous examples, the solution in this example has less smoothness. And f blows up at the boundary. As in the Example 3, we choose N=25,81,289,1089,4225 Halton data sites which are randomly distributed in the interior domain but arrange $4(\sqrt{N}-1)$ equidistant points on the boundary. Tables 7-8 provide the L^2 error and convergence rate of one-level collocation and multilevel collocation respectively. We can observe that the convergence rates of one-level and multilevel collocation are still quite higher even for the solution which has less smoothness. Figs. 7-8 show the fill plots of the numerical solutions for different frequencies.

6.5 Example 5 (constant wave speed)

We now present a numerical example outside of our convergence theory. We take $c(x,y)=1$ and $f(x,y)=0$. The computational solutions of one-level and multilevel collocation for different frequencies are displayed in Figs. 9 and 10, respectively. Fig. 11 shows the computational results of the finite element method with rectangular mesh. These results are obtained by using COMSOL Multiphysics software. It is very close to the sim-

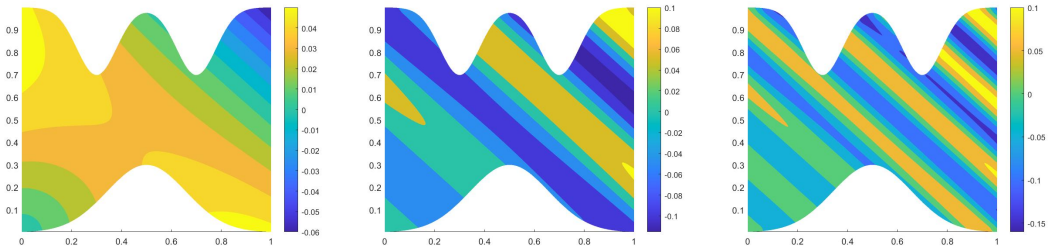

(a) $\omega=1$ (b) $\omega=10$ (c) $\omega=20$

Figure 7: The real part of the one-level numerical solution for different frequencies, when $N=1089$ on M-shaped duct.

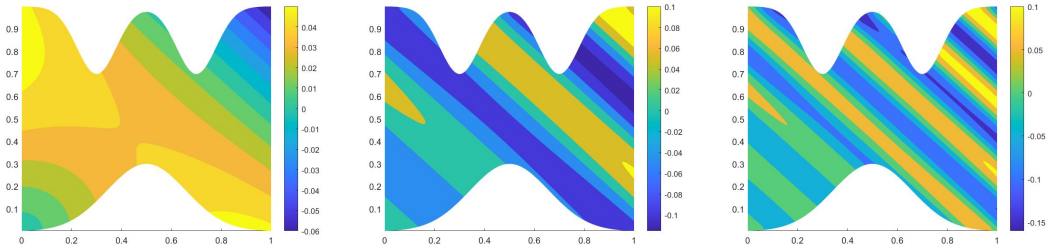

(a) $\omega=1$ (b) $\omega=10$ (c) $\omega=20$

Figure 8: The real part of the multilevel numerical solution for different frequencies, when $N=1089$ on M-shaped duct.

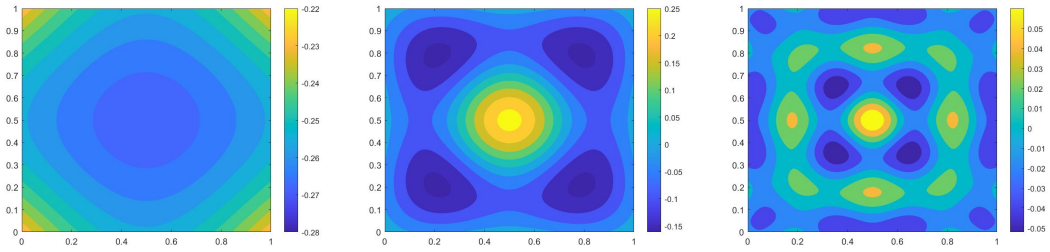

(a) $\omega=1$ (b) $\omega=10$ (c) $\omega=20$

Figure 9: The real part of the one-level numerical solution of Example 5 for different frequencies, when $N=1089$.

ulation results of one-level and multilevel collocation. The accuracy and efficiency of the proposed methods are validated again.

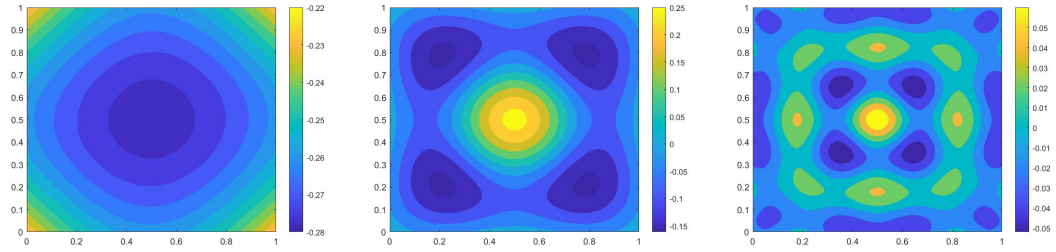

(a) $\omega=1$ (b) $\omega=10$ (c) $\omega=20$

Figure 10: The real part of the multilevel numerical solution of Example 5 for different frequencies, when $N=1089$.

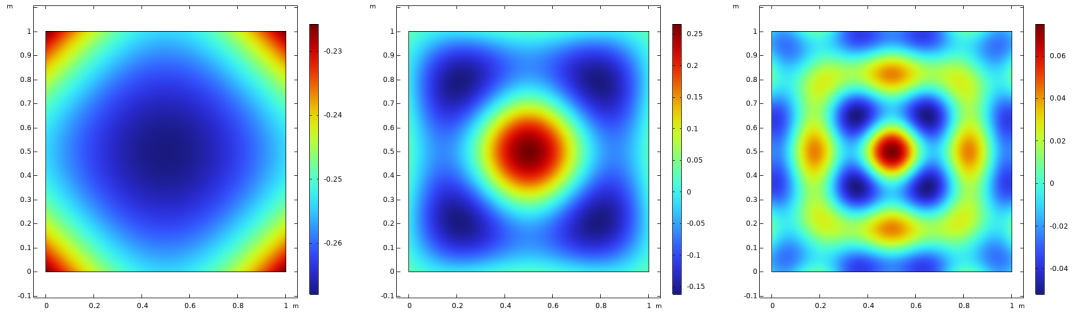

(a) $\omega=1$ (b) $\omega=10$ (c) $\omega=20$

Figure 11: The real part of the FEM solution of Example 5 for different frequencies, when $h=1/32$.

7 Conclusions

The paper developed one-level and multilevel RBF collocation methods for solving the Helmholtz equation with variable wave speed and provided convergence proofs. The theoretical convergence was established by using the regularity theory of the solution, the sampling inequality, and the approximation property of the radial basis functions trial spaces. The results in the paper are obtained based on the symmetric collocation.

For the non-symmetric collocation method, we cannot provide sufficient conditions to ensure the non-singularity of this method yet at present. Nevertheless, [29,30] show that the non-symmetric collocation method is convergent once the testing discretization has been selected to have more degrees of freedom than the trial discretization. Recently, the authors have proved the L^2 convergence of the one-level non-symmetric collocation method for the second order elliptic boundary value problems [24,25]. The convergence proofs there is different from the theory in the present paper, which mainly depends on the inverse inequality satisfied by the functions from kernel-based trial space. The convergence order of the non-symmetric collocation method is only $h^{\sigma-2-d/2}$. It is currently not yet optimal and deserve refinement.

In addition, we did not consider iterative methods for solving the linear system (4.6a)-(4.6b). In the future work, we will develop effective iterative methods and preconditioning techniques to solve the linear system which is produced by the symmetric RBF collocation.

Acknowledgements

This work was supported by National Natural Science Foundations of China (Nos. 12561074, 12061057 and 12202219), the Natural Science Foundations of Ningxia Province (Nos. 2023AAC05001 and 2024AAC02009), the Ningxia Youth Top Talents Training Project, and the Ningxia Higher Education Science Research Project (No. NYG2022004).

References

[1] R. ADAMS, AND P. FOURNIER, Sobolev Spaces, Pure and Applied Mathematics, 2nd ed.; Academic Press: New York, NY, USA, (2003).

[2] A. AZIZ, R. KELLOGG, AND A. STEPHENS, *A two point boundary value problem with a rapidly oscillating solution,* Numer. Math., 1-2 (1988), pp. 107–121.

[3] R. BALAM, AND M. ZAPATA, *A new eighth-order implicit finite difference method to solve the three-dimensional Helmholtz equation,* Comput. Math. Appl., 80 (2020), pp. 1176–1200.

[4] S. BRENNER, AND L. SCOTT, The Mathematical Theory of Finite Element Methods, 3nd ed.; Springer, New York, (2008).

[5] D. BROWN, D. GALLISTL, AND D. PETERSEIM, *Multiscale Petrov-Galerkin method for high frequency heterogeneous Helmholtz equations,* Meshfree Methods for Partial Differential Equations VIII, Lect. Notes Comput. Sci. Eng., vol. 115, Springer, (2017), Cham., 85–115.

[6] C. CHEN, M. GANESH, M. GOLBERG, AND A. H. D. CHENG, *Multilevel compact radial functions based computational schemes for some elliptic problems,* Comput. Math. Appl., 43 (2002), pp. 359–378.

[7] A. CHERNIH, AND Q. T. LE GIA, *Multiscale methods with compactly supported radial basis functions for elliptic partial differential equations on bounded domains,* ANZIAM J., 54 (2012), pp. C137–C152.

[8] A. CHERNIH, AND Q. T. LE GIA, *Multiscale methods with compactly supported radial basis functions for the Stokes problem on bounded domains,* Adv. Comput. Math., 42 (2013), pp. 1187–1208.

[9] A. CHERNIH, AND Q.T. LE GIA, *Multiscale methods with compactly supported radial basis functions for Galerkin approximation of elliptic PDEs,* IMA J. Numer. Anal., 34 (2014), pp. 569–591.

[10] H. DASTOUR, AND W. LIAO, *A fourth-order optimal finite difference scheme for the Helmholtz equation with PML,* Comput. Math. Appl., 78 (2019), pp. 2147–2165.

[11] H. DASTOUR, AND W. LIAO, *A generalized optimal fourth-order finite difference scheme for a 2D Helmholtz equation with the perfectly matched layer boundary condition,* J. Comput. Appl. Math., 39 (2021), 113544.

[12] P. FARRELL, AND H. WENDLAND, *RBF multiscale collocation for second order elliptic boundary value problems,* SIAM J. Numer. Anal., 51 (2013), pp. 2403–2425.
[13] P. FARRELL, K. GILLOW, AND H. WENDLAND, *Multilevel interpolation of divergence-free vector fields,* IMA J. Numer. Anal., 37 (2017), pp. 332–353.
[14] G. FASSHAUER, *Solving partial differential equations by collocation with radial basis functions,* in: A. Méhauté, C. Rabut, and L. Schumaker, (eds.), Surface Fittingand Multiresolution Methods, pp. 131–138. Vanderbilt University Press, Nashville, (1997).
[15] G. FASSHAUER, *Solving differential equations with radial basis functions: multilevel methods and smoothing,* Adv. Comput. Math., 11 (1999), pp. 139–159.
[16] I. GRAHAM, O. PEMBERY, AND E. SPENCE, *The Helmholtz equation in heterogeneous media: A priori bounds, well-posedness, and resonances,* J. Differential Equations, 266 (2019), pp. 2869–2923.
[17] I. GRAHAM, AND S. SAUTER, *Stability and finite element error analysis for the Helemholtz equation with variable coefficients,* Math. Comput., 89(321) (2020), pp. 105–138.
[18] U. HETMANIUK, *Stability estimates for a class of Helmholtz problems,* Commun. Math. Sci., 5(3) (2007), pp. 665–678.
[19] Y. HON, AND R. SCHABACK, *On unsymmetric collocation by radial basis functions,* J. Appl. Math. Comput., 119 (2001), pp. 177–186.
[20] E. KANSA, *Application of Hardy's multiquadric interpolation to hydrodynamics,* in Proceedings of the 1986 Annual Simulations Conference, Vol. 4, (1986), San Diego, CA, 111–117.
[21] D. LAFONTAINE, E. SPENCE, AND J. WUNSCH, *Wavenumber-explicit convergence of the hp-FEM for the full-space heterogeneous Helmholtz equation with smooth coefficients,* Comput. Math. Appl., 113 (2022), pp. 59–69.
[22] E. LARSSON, AND U. SUNDIN, *An investigation of global radial basis function collocation methods applied to Helmholtz problems,* Dolomites Research Notes on Approximation, 13 (2020), pp. 65–85.
[23] Q. T. LE GIA, I. SLOAN, AND H. WENDLAND, *Multiscale RBF collocation for solving PDEs on spheres,* Numer. Math., 121 (2012), pp. 99–125.
[24] Z. LIU, AND Q. XU, *L^2 error estimates of unsymmetric RBF collocation for second order quasilinear elliptic equations,* Commun. Nonlinear Sci. Numer. Simulat., 127 (2023), 107563.
[25] Z. LIU, AND Q. XU, *L^2 error estimates of unsymmetric RBF collocation for second order elliptic boundary value problems,* Results Appl. Math., 23 (2024), 100495.
[26] C. LOEFFLER, R. GALIMBERTI, AND H. BARCELOS, *A self-regularized Scheme for solving Helmholtz problems using the boundary element direct integration technique with radial basis functions,* Eng. Anal. Bound. Elements, 118 (2020), pp. 11–19.
[27] C. RIEGER, R. SCHABACK, AND B. ZWICKNAGL, *Sampling and stability,* Mathematical Methods for Curves and Surfaces, Lecture Notes in Computer Science, vol. 5862, pp. 347–369. Springer, New York, (2010).
[28] S. SAUTER, AND C. TORRES, *Stability estimate for the Helmholtz equation with rapidly jumping coefficients,* Z. Angew. Math. Phys., 69 (2018), 139.
[29] R. SCHABACK, *Convergence of unsymmetric kernel-based meshless collocation methods,* SIAM J. Numer. Anal., 45(1) (2007), pp. 333–351.
[30] R. SCHABACK, *Unsymmetric meshless methods for operator equations,* Numer. Math., 114 (2010), pp. 629–651.
[31] N. SONG, AND E. LEE, *Dual system least squares finite element method for the Helmholtz equation,* Results Appl. Math., 9 (2021), 100138.
[32] A. TOWNSEND, AND H. WENDLAND, *Multiscale analysis in Sobolev spaces on bounded domains*

with zero boundary values, IMA J. Numer. Anal., 33 (2013), pp. 1095–1114.
[33] H. WENDLAND, Scattered Data Approximation. Cambridge University Press, Cambridge, UK, (2005).
[34] H. WENDLAND, *Multiscale analysis in Sobolev spaces on bounded domains,* Numer. Math., 116 (2010), pp. 493–517.
[35] H. WENDLAND, *Multiscale radial basis functions,* in: I. Pesenson, Q. Gia, A. Mayeli, H. Mhaskar, and D. Zhou, (eds.), Frames and Other Bases in Abstract and Function Spaces–Novel Methods in Harmonic Analysis, vol. 1, pp. 265–299. Birkhäuser, Cham., (2005).
[36] H. WENDLAND, *Solving partial differential equations with multiscale radial basis functions,* in Contemporary Computational Mathematics–A Celebration of the 80th Birthday of S. Ian, J. Dick, F. Kuo and H. Wozniakowski (eds.), Springer, Berlin, Germany, pp. 1191–1213, (2018).
[37] Z. WU, *Hermite-Birkhoff interpolation of scattered data by radial basis functions,* Approx. Theory Appl., 8 (1992), pp. 1–10.
[38] M. WILLIAM, Strongly Elliptic Systems and Boundary Integral Equations, Cambridge University Press, Cambridge, UK, (2000).
[39] J. WLOKA, Partial Differential Equations. Cambridge University Press, Cambridge, UK, (1987).